N72-28917

NASA TECHNICAL MEMORANDUM

NASA TM X-2595

NASA TM X-2595

COMPARISON OF HEAT-TRANSFER TEST DATA FOR A CHORDWISE-FINNED, IMPINGEMENT-COOLED TURBINE VANE TESTED IN A FOUR-VANE CASCADE AND A RESEARCH ENGINE

by Herbert J. Gladden and Frederick C. Yeh

Lewis Research Center

Cleveland, Ohio 44135

NATIONAL AERONAUTICS AND SPACE ADMINISTRATION • WASHINGTON, D. C. • JULY 1972

1. Report No.	2. Government Accession No.	3. Recipient's Catalog No.
NASA TM X-2595		

4. Title and Subtitle	5. Report Date
COMPARISON OF HEAT-TRANSFER TEST DATA FOR A CHORDWISE-FINNED, IMPINGEMENT-COOLED TURBINE VANE TESTED IN A FOUR-VANE CASCADE AND A RESEARCH ENGINE	July 1972
	6. Performing Organization Code

7. Author(s)	8. Performing Organization Report No.
Herbert J. Gladden and Frederick C. Yeh	E-6870
	10. Work Unit No. 764-74

9. Performing Organization Name and Address	11. Contract or Grant No.
Lewis Research Center National Aeronautics and Space Administration Cleveland, Ohio 44135	
	13. Type of Report and Period Covered
12. Sponsoring Agency Name and Address	Technical Memorandum
National Aeronautics and Space Administration Washington, D.C. 20546	14. Sponsoring Agency Code

15. Supplementary Notes

16. Abstract

The heat-transfer characteristics of a chordwise-finned, impingement-cooled vane were investigated in both a modified J-75 research engine and a four-vane cascade. The data were compared by a correlation of temperature difference ratio with coolant- to gas-flow ratio and also by two modifications of this correlation. The results indicated that the cascade vane temperature data can generally be used to represent the engine vane temperature data. A discussion of engine and cascade gas-side heat-transfer coefficients is also presented. A redesign of the vane leading edge could significantly increase the potential turbine-inlet temperature operating limit.

17. Key Words (Suggested by Author(s))	18. Distribution Statement
Turbine cooling Air-cooled vane Engine-cascade comparison Turbulence effects	Unclassified - unlimited

19. Security Classif. (of this report)	20. Security Classif. (of this page)	21. No. of Pages	22. Price*
Unclassified	Unclassified	37	$3.00

* For sale by the National Technical Information Service, Springfield, Virginia 22151

COMPARISON OF HEAT-TRANSFER TEST DATA FOR A CHORDWISE-FINNED, IMPINGEMENT-COOLED TURBINE VANE TESTED IN A FOUR-VANE CASCADE AND A RESEARCH ENGINE

by Herbert J. Gladden and Frederick C. Yeh

Lewis Research Center

SUMMARY

A comparison was made of the heat-transfer characteristics of a chordwise-finned, impingement-cooled vane tested in both a modified J-75 turbojet engine and a four-vane cascade. Experimental data were taken at gas temperatures and pressures to 1650 K (2510° F) and 29.7 newtons per square centimeter (43.1 psia) and coolant temperatures to 810 K (998° F). Higher gas pressures were also investigated in the cascade (59.0 N/cm^2; (85.6 psia)) but at a reduced gas temperature level (1540 K; (2312° F)). Both averaged and local vane midspan temperature data were correlated for a wide range of operating conditions by a temperature difference ratio (gas minus vane temperature divided by gas minus coolant temperature) plotted against the total coolant- to gas-flow ratio. Two modifications of this correlation are also presented for average cascade temperature data. The average vane midspan temperatures were correlated by these three methods to within ±5 percent.

The average correlations for the engine and the cascade were equivalent. However, comparison of temperature gradients between the leading edge and the midchord region of the engine vane and the cascade vane indicated that the engine vane had the larger gradient by about 30 K (54° F) at similar operating conditions.

The results of this study indicated the coolant flow distribution in the cascade vane was different than the coolant flow distribution in the engine vane. However, the cascade can be used to represent engine conditions. Selected experimental vane temperatures were also predicted to within 33 K (59° F) by a one-dimensional analytical approximation.

The local temperature difference ratios were utilized to compare the gas-side heat-transfer coefficient distribution around the engine vane with similar coefficients around the cascade vane. Heat-transfer coefficients compared by this method did not follow previous results shown for two other vanes because of differences in the coolant-flow distribution through the engine vane and the cascade vane.

INTRODUCTION

The heat-transfer performance of a chordwise-finned, impingement-cooled turbine vane was investigated in both a four-vane cascade and a modified J-75 turbojet engine. Data obtained from these tests are compared to illustrate the similarities and differences in performance of a turbine vane operated in different facilities.

A similar comparison of cascade and engine data is presented in reference 1 for a vane with the same gas-side airfoil profile and a similar internal cooling design. The reference 1 vane, however, had an array of film cooling holes on the suction and pressure surface just aft of the leading edge. Reference 1 concluded that temperature data obtained from a vane operated in the cascade were representative of temperature data obtained with the J-75 engine, with the exception of the vane leading edge. Methods of correlating temperature data for an air-cooled turbine vane are discussed in references 2 to 4. In each case, it was found that the ratio of gas minus vane temperature to gas minus coolant temperature plotted against the coolant- to gas-flow ratio was as good as or better than the more complicated correlations derived in reference 2. However, each of the correlations derived in reference 2 has a definite coolant temperature effect not accounted for by the correlation.

The purposes of this report are (1) to compare the performance of this vane in the cascade environment with its operation in the engine environment, (2) to compare the leading-edge gas-to-vane heat-transfer coefficients of an engine vane with those of a cascade vane, (3) to present revised methods of correlating the vane temperature data, (4) to compare the experimental vane temperatures with vane temperatures calculated by a one-dimensional approximation of the heat flux, and (5) to evaluate the cooling design of this turbine vane.

Cascade tests were run over the following ranges of conditions: inlet gas temperatures and pressures to 1650 K (2510° F) and 57.3 newtons per square centimeter (86 psia), inlet coolant temperatures to 810 K (998° F), and coolant- to gas-flow ratios from 0.019 to 0.129. Engine tests were run for similar conditions. Turbine-inlet temperatures and pressures were run to 1650 K (2510° F) and 32 newtons per square centimeter (46.5 psia), respectively. Coolant inlet temperatures ranged to 700 K (800° F); the coolant- to gas-flow ratio ranged from 0.027 to 0.127.

SYMBOLS

A_r area ratio

A_s surface area

a, b constants

b_{es} equivalent slot width

c_p specific heat

d vane leading-edge diameter

d_h hydraulic diameter

d_n nozzle diameter

g acceleration due to gravity

h heat-transfer coefficient

J mechanical equivalent of heat

k thermal conductivity

L overall suction- or pressure-surface distance

m_x area weighting factor

p pressure

Re Reynolds number

T temperature

v velocity

$\dot{w}$ flow rate

x surface distance from stagnation point

Z hole-to-surface spacing

γ specific-heat ratio

η_f fin effectiveness

η_t thermal effectiveness

Λ recovery factor

φ temperature difference ratio

Subscripts:

c coolant

calc calculated

cas cascade

ci coolant inlet

co coolant outlet

eng engine

g gas

ge effective gas

max maximum

meas measured

mod modified

ref reference

s static

Ti turbine inlet

w vane wall

x local

Superscripts:

– average

' total

APPARATUS

Cascade Description

The cascade facility was designed for continuous operation at gas conditions of 1650 K (2510° F) and 110 newtons per square centimeter (160 psia). A detailed description of the facility is presented in reference 5. The test section was an annular sector of a vane row and contained four vanes and five flow channels. A plan view of the cascade test section is shown schematically in figure 1(a). A photograph of the installed vane pack is shown in figure 1(b). The two central vanes shown in figure 1(b) were test vanes. The two test vanes were supplied by a common cooling-air system and the cooling air from this system could be preheated to approximately 920 K (1196° F) to simulate compressor bleed air temperature. The two outer vanes, used to provide flow channels for the test vanes and to serve as radiation shields between the test vanes and the water-cooled cascade walls, were each supplied by a separate cooling-air supply system.

For low-gas-temperature tests, the main burner section was replaced by a spool piece, and combustion gas was then supplied to the test section by an auxiliary burner system located upstream from the main burner. The main burner supplied combustion gas at temperatures from 920 to 1650 K (1196° to 2510° F), while the auxiliary burner

supplied combustion gas at temperatures to 920 K (1196° F). Reference 2 shows a schematic of the auxiliary burner system.

Engine Description

The research engine used in this investigation was a modified high-pressure spool and combustor assembly of a two-spool J-75 turbojet engine. A detailed description of the engine facility is given in reference 5. A schematic of the turbine section of the engine is shown in figure 2. The major feature of the test engine was the provision for two separate and distinct cooling-air systems in the stator assembly and a similar dual air supply system for the turbine rotor.

The complete turbine stator assembly consisted of 72 vanes. In the research engine, provision was made for a group of five vanes to be installed adjacent to each other; these five vanes were the test vanes and were supplied cooling air from a laboratory air system independent of the system which supplies cooling air to the remaining 67 slave vanes. A similar arrangement also existed for the rotor and rotor blades.

Vane Description

A cutaway drawing of the vane design tested in both the engine and the cascade is shown in figure 3. The vane span was 10.2 centimeters (4 in.), and the midspan chord length was 6.3 centimeters (2.5 in.). Cooling air entered the vane from the supply tube located at the tip or outer diameter of the vane and was ducted into a central cavity as shown. The central cavity acted as a plenum chamber for the cooling air before it was distributed to a series of impingement holes in the forward portion of the plenum and to a series of chordwise-finned passages with entrances just aft of the impingement hole partition.

A row of 46 impingement holes of 0.127-centimeter (0.050-in.) diameter and spaced 0.203 centimeter (0.080 in.) center to center was used to impingement cool the vane leading edge; these holes were located 0.51 centimeter (0.20 in.) from the inside surface of the vane leading-edge. Approximately 30 percent of the cooling air, after impinging on the internal leading-edge surface, flowed chordwise adjacent to the vane suction and pressure surfaces into spanwise collecting passages. This cooling air then flowed toward the vane hub and exhausted into a plenum below the hub platform. This air stream then entered the gas stream between the vane and blade row of the engine and, in the cascade, just aft of the vane hub platform trailing edge. The cooling air not used for impingement cooling of the leading edge entered a series of chordwise-finned passages adjacent to the vane suction and pressure surfaces at a point 1.91 centi-

meters (0.75 in.) from the vane leading edge. The finned passages were nominally 0.076 centimeter (0.030 in.) square. The coolant flowed through these channels and exited through a split trailing edge. The trailing-edge spacing was maintained by five spacers, 0.25 centimeter (0.1 in.) wide and about 0.05 centimeter (0.02 in.) high, which formed six flow channels.

Vane Fabrication

For the heat-transfer tests described in this report, only a small number of vanes of the type tested were required. As a result, no attempt was made to develop a procedure for mass producing the vanes. The fabrication techniques are discussed in references 3 and 4.

INSTRUMENTATION

For the cascade tests, each of the two test vanes was instrumented with 25 Chromel-Alumel thermocouples embedded in the walls of the airfoils. Thirteen of these were located at the vane midspan, and six each at the hub and tip sections. For the engine tests, there were three instrumented vanes in the five test vane pack. A total of 25 thermocouples were also used; fourteen were located at the vane midspan section, four at the hub, and seven at the tip. Because of space limitations the maximum number of thermocouples installed on any one vane in the engine was seven. For convenience, and for comparison purposes with results from the cascade tests, a composite of the midspan engine vane thermocouple locations is shown in figure 4. The cascade vanes and the engine composite vane had the same number of thermocouples installed in identical positions.

The construction of the thermocouples is discussed in reference 6.

Cooling-air temperature and pressure were measured at the inlet to the vanes. The turbine-inlet conditions of the cascade and the engine were measured by radially traversing probes. These and other operational instrumentation are discussed in reference 5.

TEST PROCEDURE

Cascade Tests

Cascade tests were run over the range of operating conditions given in table I. The operating procedure is described in this section. After burner ignition, the desired

combustion gas-flow rate and pressure were established by adjusting inlet and exhaust throttle valves while maintaining the desired total temperature by an automatic controller. The combustion gas-flow rate was adjusted until the desired exit static- to total-pressure ratio was attained. A midspan, midchannel Mach number of 0.85 was maintained for these tests. For control purposes, the hub and tip exit static pressures were averaged, and the average was divided by the inlet total pressure (assumed equal to the exit total pressure). When the desired combustion gas conditions were established, the coolant-flow rate was varied in a stepwise manner at a given coolant inlet temperature. The coolant- to gas-flow ratio ranged from about 0.019 to 0.129.

Several of the cascade data points were established based on the similarity consideration of reference 7. Data points were taken at a turbine-inlet temperature and pressure of 760 K (909° F) and 12.95 newtons per square centimeter (18.8 psia) and a coolant inlet temperature of 310 K (98° F). Based on the procedure of reference 7, these gas and coolant conditions were scaled to a turbine-inlet temperature and pressure of 1540 K (2312° F) and 29.5 newtons per square centimeter (42.8 psia) and a coolant inlet temperature of 600 K (620° F). Experimental data were taken at both sets of conditions.

Engine Tests

Engine tests were run over the range of operating conditions given in table II. A test series consisted of a group of test points made at a given nominal coolant inlet temperature. The normal operating procedure was to start a series of test points with the highest coolant flow rate to the vanes (and blades, if they were also being tested). During most of the testing, the slave vanes and blades were overcooled to preserve life. The test vane coolant flows were reduced in incremental steps until a maximum vane temperature of about 1280 K (1844° F) was reached (this was considered the maximum safe operating vane temperature). Coolant- to gas-flow ratios ranged from 0.027 to 0.127. For simultaneous testing of vanes and blades, combined changes in vane and blade coolant-flow rates resulted in small changes in engine speed in order to reestablish the desired nominal average turbine-inlet temperature; for some series of tests, the engine speed varied as much as 200 to 500 rpm.

Determination of Coolant-Flow Distribution

A determination of the coolant-flow distribution in the vane investigated is discussed in this section. First, the total flow through the vane was measured for a series of inlet pressures from 3.4 to 27.6 newtons per square centimeter (5 to 40 psig). The

leading- and trailing-edge exit ports were open to the atmosphere. Next, the trailing-edge exit port was closed, and the flow through the leading edge of the vane was measured for the same series of inlet pressures. Finally, the leading-edge exit port was closed, the trailing-edge exit port opened, and the procedure repeated. The results of these tests are presented in reference 8.

ANALYSIS METHODS

Experimental Data Correlations

Several methods of correlating vane and blade heat-transfer data were developed in references 2 to 4. These references show that a plot of the temperature difference ratio φ against coolant- to gas-flow ratio $\dot{w}_c/\dot{w}_g$ is as accurate as the more detailed correlations of reference 2. The temperature difference ratio is defined in equation (1):

$$\varphi = \frac{T_{Ti} - T_w}{T_{Ti} - T_{ci}} \tag{1}$$

For convenience, the turbine-inlet temperature and the coolant inlet temperature were used in the correlation in place of local or average values. An integrated average midspan vane temperature $\overline{T}_w$ was used to define an average temperature difference ratio. Local temperature difference ratios were found by using local wall temperatures.

This simplified correlation showed progressively greater error with decreasing coolant flow for the vane discussed in reference 2. It was speculated that this was the effect of using the coolant inlet temperature in the correlations instead of the local coolant temperature. It was also apparent by studying this correlation that the data were separated by coolant inlet temperature.

Because of these observations, two empirical modifications of the correlation are presented as alternative means of reducing the error associated with this type of correlation. The first modification employs the thermal effectiveness parameter η_t discussed in reference 9:

$$\eta_t = \frac{T_{co} - T_{ci}}{\overline{T}_w - T_{ci}} \tag{2}$$

If the temperature difference ratio φ is redefined so that it is based on the average coolant temperature instead of the inlet coolant temperature, a modified temperature

difference ratio can be obtained:

$$\overline{\varphi}_{mod} = \frac{T_{Ti} - \overline{T}_w}{T_{Ti} - \frac{1}{2}(T_{co} + T_{ci})}$$

$$= \left[1 + \left(\frac{1 - \eta_t}{2}\right)\left(\frac{\overline{T}_w - T_{ci}}{T_{Ti} - \overline{T}_w}\right)\right]^{-1} \tag{3}$$

Reference 10 has shown η_t to be inversely proportional to a power of the coolant Reynolds number.

An alternative method of calculating the thermal effectiveness was utilized for this report. This method is based on the integrated total heat input to the vane and the total coolant flow

$$T_{co} - T_{ci} = \frac{A_s \sum_x h_{g,x}(T_{ge,x} - T_{w,x})m_x}{\left(\sum_x m_x\right)\dot{w}_c c_p} \tag{4}$$

where m_x is an area weighting value assigned to each thermocouple location. Equation (2) can also be rewritten as follows to obtain an experimental value of the thermal effectiveness:

$$\eta_t = \frac{A_s \sum_x h_{g,x}(T_{ge} - T_{w,x})m_x}{\sum_x m_x(T_w - T_{ci})\dot{w}_c c_p} \tag{2a}$$

The gas-side heat-transfer coefficients were calculated by using a turbulent flat plate equation or a potential flow cylinder equation as required.

Reference 2 presents two equations for turbulent flow over the gas side of a vane. For the leading edge, the correlation for flow past a cylinder was used:

$$h_g = \frac{k_g}{d_g} 1.14 Re_g^{0.5} Pr_g^{0.4} \left(1 - \left|\frac{\theta}{90^o}\right|^3\right) \tag{5}$$

where θ is the angle measured from the stagnation point and $-80^o < \theta < 80^o$. For the other sections of the vane, the correlation for turbulent flow over a flat plate was used:

$$h_{g,x} = \frac{k_g}{x} 0.0296 Re_{g,x}^{0.8} Pr^{1/3} \tag{6}$$

Properties used in equations (5) and (6) were based on the following reference temperature:

$$T_{ref} = 0.28T_s + 0.5T_w + 0.22T_{ge} \tag{7}$$

A second modification, to reduce the spread of data due to coolant temperature, is based on the coolant- to wall-temperature ratio. A similar approach was used in reference 11 to correlate turbulent gas heat-transfer coefficients. The temperature difference ratio was correlated by plotting $\overline{\varphi}$ against $(\dot{w}_c/\dot{w}_g)\sqrt{T_{ci}/\overline{T}_w}$.

Comparison of Engine and Cascade Gas-to-Vane Heat-Transfer Coefficients

Engine and cascade gas-to-vane heat-transfer coefficients were compared in reference 1. These coefficients were first compared by utilizing the experimental pressure distribution obtained in each facility and then by utilizing the experimental local temperature difference ratios. An equation was developed in reference 1 which permitted the calculation of the ratio $h_{g,eng}/h_{g,cas}$ from the experimental static- to total-pressure ratio distribution around the vane:

$$\frac{h_{g,eng}}{h_{g,cas}} = \frac{(\rho v)_{g,eng}^{0.8}}{(\rho v)_{g,cas}^{0.8}} = \left[\frac{\left(\frac{p_x}{p'_{Ti}}\right)_{cas}^{(\gamma-1)/\gamma} \sqrt{1 - \left(\frac{p_x}{p'_{Ti}}\right)_{eng}^{(\gamma-1)/\gamma}}}{\left(\frac{p_x}{p'_{Ti}}\right)_{eng}^{(\gamma-1)/\gamma} \sqrt{1 - \left(\frac{p_x}{p'_{Ti}}\right)_{cas}^{(\gamma-1)/\gamma}}}\right]^{0.8} \tag{8}$$

This equation was developed by assuming the temperature and pressure level of the engine and the cascade were equal and that the heat-transfer coefficients depend only on the Reynolds number.

The temperature difference ratio can also be defined as a function of the heat-transfer coefficients:

$$\varphi = \frac{1}{1 + A_r \frac{h_g}{h_c}} \tag{9}$$

When $h_{c,eng}$ and $h_{c,cas}$ are equated, the following ratio is obtained whereby the local gas-side heat-transfer coefficient of the engine vane and cascade vane can be compared by utilizing experimental temperature data:

$$\frac{h_{g,eng}}{h_{g,cas}} = \left(\frac{\varphi}{1 - \varphi}\right)_{cas} \left(\frac{1 - \varphi}{\varphi}\right)_{eng} \tag{10}$$

Obviously, the gas temperature, pressure, and Reynolds number and the coolant temperature, pressure, and Reynolds number should be equal to make a valid comparison with this equation. Any inequality of cascade and engine conditions will adversely influence the comparison.

One-Dimensional Approximation of Vane Wall Temperature

The following procedure was used to calculate the vane wall temperature for a given set of conditions. The calculation procedure was based on a one-dimensional approximation of heat transferred through the wall of the vane. Substituting the definition of the temperature difference ratio in equation (9) and rearranging give the following equation for the wall temperature:

$$T_{w,x} = \frac{T_{ci} + T_{ge,x} A_{r,x} \frac{h_{g,x}}{h_{c,x}}}{1 + A_{r,x} \frac{h_{g,x}}{h_{c,x}}} \tag{11}$$

The local wall temperature can be calculated by determining the gas-side and coolant-side heat-transfer coefficients, the area ratio, and the effective gas temperature at the desired locations around the vane. The gas-side heat-transfer coefficients can be determined from equation (5) or (6). Reference 1 presents correlations which can be used to determine coolant-side heat-transfer coefficients. For impingement cooling

$$h_c = \frac{k_c}{d_n} 0.0364 Re_c^{0.62_x - 0.475} \tag{12}$$

where the Reynolds number is based on the nozzle diameter. For turbulent convection cooling in the finned passages

$$h_c = \frac{k_c}{d_n} \eta_f 0.021 Re_c^{0.8} Pr_c^{0.333} \tag{13}$$

where η_f is equal to 3.08 (see ref. 1) and is the fin effectiveness for the midchord region of this vane. For laminar convection cooling in the finned passages

$$h_c = \frac{k_c}{d_n} \eta_f 3.66 \tag{14}$$

The effective gas temperature can be determined by equation (15):

$$T_{ge} = T'_g - (1 - \Lambda) \frac{v_g^2}{2gJc_p} \tag{15}$$

Vane Potential

The potential operating limits of the vane can be determined by utilizing the φ_x curve fit equation as found for the vane hotspot. If a maximum allowable wall temperature is assumed, the allowable turbine-inlet temperature can be calculated as a function of the coolant- to gas-flow ratio and the coolant temperature. The φ_x correlation can be expressed as

$$T_{Ti} = T_{w,max} + \left(\frac{\dot{w}_c}{\dot{w}_g}\right)^a \frac{T_{w,max} - T_{ci}}{b} \tag{16}$$

The constants a and b are found by a least squares curve fit.

RESULTS AND DISCUSSION

Comparison of Gas Temperature Profiles

The measured turbine-inlet temperature profiles for the engine and the cascade are shown in figure 5. The cascade data shown are representative of the gas temperature in front of channel 3 (see fig. 1). Spanwise distributions for both the high-temperature burner and the low-temperature burner are designated by the square symbols. The engine data shown were measured by eight circumferentially spaced probes that were traversed in a radial direction. Corresponding radial positions on each of the eight probes were averaged to obtain the profile shown in figure 5. Since the test vanes in the engine were not located directly behind the traversing probes, the vanes may have been subjected to a different gas temperature profile than that shown in the figure.

Comparison of the high-temperature profiles of figure 5 indicates that the cascade had a higher ratio of maximum to average gas temperature than the engine. This was partially due to the water-cooled housing of the cascade. Because of this phenomenon, the hub and tip region of the cascade vanes operated at a lower temperature level than the engine vanes. Consequently, the cascade vanes were subject to greater radial conduction loss at the midspan than were the engine vanes.

Comparison of Chordwise Temperature Distributions

Chordwise temperature distributions for the vanes tested in the cascade and the engine are shown in figure 6. These data are for nominally similar operating conditions for the two test facilities and are approximate design conditions. The design conditions for these vanes were a turbine-inlet temperature of 1533 K (2300° F), a coolant inlet temperature of 589 K (600° F), and a coolant- to gas-flow ratio of 0.05.

Comparing the two profiles, it is noted that the leading-edge and suction-surface temperature levels of the two vanes were quite similar but the engine vane leading edge was up to 30 K (54° F) hotter than the cascade vane. The pressure-surface region of the engine vane was up to 90 K (162° F) hotter than the cascade vane. These temperature

differences between the engine vane and the cascade vane could be attributed to differences in coolant distribution between the vanes or to a variation in the turbine-inlet temperature that each of the five vanes in the engine "sees." The leading-edge flow exhausts into a plenum at the vane hub region which, in turn, is vented to the gas stream aft of the vane row. The method of venting into the gas stream is somewhat different in the cascade from that in the engine. As a result, the leading-edge coolant flows can be different for the same inlet flow and result in different coolant-flow distributions in the cascade and the engine. Reduced flow to the leading edge of the cascade vane could lead to the results shown. The results of reference 1 (see fig. 7) indicate that the aft portion of the two vanes should be at about the same temperature, while the leading edge of the engine vane is considerably hotter than the cascade vane. Reference 1 attributes this phenomenon to the higher turbulence level of the engine environment. This is discussed further in the section Comparison of Engine and Cascade Gas-Side Heat-Transfer Coefficients.

Figure 7 is a reprint of the comparison of chordwise temperature distributions for the cascade and the engine vanes of reference 1. A cross-sectional view is included in figure 7 to illustrate the coolant-flow paths and the thermocouple locations. Two coolant- to gas-flow ratios are shown, that is, 0.05 and 0.08. The reference 1 vane was similar in design to the vane of this report except that the cooling air that impingement cooled the leading edge was exhausted through spanwise film cooling holes located on both the suction and the pressure surfaces. Because the leading-edge cooling air exhausted directly into the gas stream, the back pressure at the vane hub, as discussed in this section, did not affect the reference 1 vane. A more detailed comparison of the vane of this report and the reference 1 vane is presented in reference 8.

Also of importance is the maximum to minimum temperature difference that existed between the leading edge and the midchord regions. Referring to figure 6, the cascade vane had a temperature difference of 300 K (540° F), whereas the engine vane had a temperature difference of 330 K (595° F).

Since the leading-edge region was impingement cooled, and because the ratio of equivalent slot width to surface distance Z/b_{es} was not optimized, the leading-edge region was essentially undercooled. The ratio Z/b_{es} was approximately 8 for this vane. Reference 12 has shown an optimum Z/b_{es} to be of the order of 2 or 3. A redesign of this vane leading-edge geometry to correct this deficiency could significantly reduce the thermal gradient that existed in the chordwise direction (to about 61 K; 110° F) (see ref. 8).

Three calculated wall temperatures are also shown in figure 6, and these temperatures were calculated for the cascade vane conditions only. These temperatures were determined by the one-dimensional approximation discussed in the section ANALYSIS METHODS. These particular locations were selected as being the most representative

of one-dimensional heat flow. However, at the leading edge, this assumption is invalid and can result in calculated temperatures much higher than if heat conduction were considered. Coolant-flow calibrations indicated the total coolant-flow distribution was approximately 30 percent to the leading edge and 70 percent to the trailing edge (see ref. 8). Three wall temperatures were estimated by use of equation (11) and this flow split.

The comparison of experimental and these calculated temperatures shows that the greatest deviation between these values was in the midchord region, where the calculated values were about 33 K (59° F) higher. The calculated leading-edge temperature was 11 K (20° F) higher than the experimental. If an uncertainty of ±10 percent is assigned to both the gas-side and the coolant-side heat-transfer coefficients, the resulting error bands on the calculated wall temperatures will easily encompass the experimental temperatures.

Comparison of Average Temperature Difference Ratio

The average temperature difference ratio $\overline{\varphi}$ for engine operating conditions is shown as a function of the coolant- to gas-flow ratio in figure 8. The data spread is by coolant temperature where, for a given coolant- to gas-flow ratio, the temperature difference ratio $\overline{\varphi}$ increases as the coolant temperature increases. A similar trend is noted in references 1 to 4. A least square curve fit of the data resulted in the equation

$$\overline{\varphi} = \frac{1}{1 + 0.18\left(\frac{\dot{w}_c}{\dot{w}_g}\right)^{-0.55}} \tag{17}$$

Figure 9(a) is a plot of the average temperature difference ratio as a function of the coolant- to gas-flow ratio for cascade operating conditions. The data spread and the least square curve fit equation are the same as the engine data results. Comparison of the curve fit equations indicates that no differences existed in the average temperature data of the engine and the cascade vane. This conclusion is biased because a greater range of coolant temperature data was included in the cascade data correlation. The effect of this greater range of coolant temperatures is to increase the $\overline{\varphi}$ value for a given coolant- to gas-flow ratio.

Modification of Average Temperature Difference Ratio

Two modifications of the average temperature difference ratio are shown in figures 9(b) and (c). The average temperature difference ratio shown in figure 9(b) was converted to an average coolant temperature basis, by using equations (3) and (4), instead of an inlet coolant temperature basis as used in figure 9(a). The least square curve fit equation of these data is

$$\overline{\varphi}_{mod} = \frac{1}{1 + 0.20\left(\frac{\dot{w}_c}{\dot{w}_g}\right)^{-0.41}} \tag{18}$$

The purpose of this modification is to reduce the error associated with the correlation as the coolant- to gas-flow ratio changes. The results of reference 2 indicated an increasing error with a decreasing coolant- to gas-flow ratio and suggested that the inlet coolant temperature became less representative of the average coolant temperature as the coolant flow decreased. The intended improvement of the correlation of the temperature data is not clearly shown by this figure.

The average temperature difference ratio $\overline{\varphi}$ as a function of a modified coolant-to gas-flow ratio $\dot{w}_c/\dot{w}_g \sqrt{T_{ci}/\overline{T}_w}$ is shown in figure 9(c). Again a correlation of the data is made by a least squares curve fit:

$$\overline{\varphi} = \frac{1}{1 + 0.13\left(\frac{\dot{w}_c}{\dot{w}_g}\sqrt{\frac{T_{ci}}{\overline{T}_w}}\right)^{-0.60}} \tag{19}$$

The purpose of this correlation was to eliminate the coolant temperature dependence noted in references 1 to 4. Comparison of the data in figure 9(c) with the data in figure 9(a) shows a reduction in the spread of the data with the inclusion of the temperature ratio term $\sqrt{T_{ci}/\overline{T}_w}$.

The modified correlations just discussed were used for cascade vane data only; however, similar results would be expected with engine vane data. These methods can also be applied to correlation of local temperature data, but such correlations are not presented in this report.

Comparison of Measured and Calculated Average Wall Temperatures

The averages of experimentally measured wall temperatures are compared with calculated average wall temperatures by using the correlation equations of the previous section. These temperature comparisons are shown in figure 10 and are presented to show the temperature data scatter associated with the correlations.

In general, the majority of the data shown in all three figures fall within a ±5 percent scatter band. Study of the individual data points in figures 10(a) and (b) indicates the modification to an average coolant temperature basis for $\overline{\varphi}$ results in little or no improvement in the ability to calculate the average wall temperature. For a given set of conditions as the coolant flow decreases, the wall temperature increases. Comparison of high and low coolant flow values in figure 10(b) shows that, in general, a better correlation is obtained at high coolant-flow rates.

Investigation of figure 10(c), however, shows that the experimental and the calculated average wall temperatures compare more favorably for the majority of data points than in the previous two cases. The added complexity of this correlation for the limited improvement in the calculated wall temperature makes use of this correlation somewhat less desirable than use of the unmodified correlation.

Cascade Local Temperature Difference Ratio Correlations

Some φ_x data and correlation equations are presented in figure 11 for the cascade vane. A representative range of data is shown in each figure along with the least squares curve fit equation. The relative position of the thermocouple is shown by the insert in each figure. The trends of these data are similar to those trends noted for the $\overline{\varphi}$ correlation, that is, the data generally separate by coolant temperature level.

Comparison of Engine and Cascade Local Temperature Difference Ratio Correlations

Selected φ_x data and correlation equations for the engine vane are presented in figure 12. Also shown in the figure are the correlation curves obtained for similar thermocouple positions on the cascade vane. The relative position of the thermocouple is shown by the insert in each figure. The solid curve correlates the engine data, while the dashed curve represents the correlated cascade data presented in figure 11. The results shown in this figure are representative of all thermocouple locations on the engine and the cascade vanes. A favorable comparison was found at all locations except the pressure surface, where the comparison suggests higher temperatures for the

engine vane. This is consistent with the chordwise temperature profile shown in figure 6.

Comparison of Engine and Cascade Gas-Side Heat-Transfer Coefficients

The gas-side heat-transfer coefficients around the engine vane and the cascade vane can be compared by using values of experimental temperature difference ratio φ and equation (10). This equation results in a ratio of engine to cascade heat-transfer coefficients. This equation is valid, however, only if the coolant temperatures, pressures, and Reynolds numbers (coolant flow rates) are equal for the two vanes and if the gas temperatures, pressures, and Reynolds numbers are equal.

The ratios of heat-transfer coefficients for three vanes tested in the engine and the cascade are shown in table III. The vane of this report and the reference 1 vane had comparable thermocouples at the stagnation point and $\pm 60^{\circ}$ from the stagnation point. The reference 2 vane had comparable thermocouples at the stagnation point and also $\pm 45^{\circ}$ from the stagnation point. The vanes of reference 1 and 2 indicate similar results, particularly at the stagnation point, where the ratio was 1.30 for both vanes. The ratio for the vane of this report varied from 0.80 to 1.05 for the locations compared.

Typical chordwise temperature profiles for the reference 2 engine vane and cascade vane are shown in figure 13. A cross-sectional view of this vane is included in figure 13 to illustrate the coolant-flow paths and the thermocouple locations. The general trends of the profile comparison shown by this figure are the same as in the profile comparison shown in figure 7 for the reference 1 vane, namely, similar temperatures over the vane surface except the leading edge, where the engine vane was hotter.

Heat-transfer coefficients were found for a cylinder installed in both a wind tunnel and an air turbine and reported in reference 13. The correlations of this reference indicate the leading-edge coefficients of an air turbine vane should be 20 percent higher than a similar coefficient for a wind tunnel vane. This increase in the coefficients is for a Reynolds number of 2×10^4, which is representative of the inlet to the cascade. Reference 1 reports an increase of 30 percent in the leading-edge heat-transfer coefficient of the engine vane compared to the cascade vane and attributes this increase to higher turbulence levels in the engine. Because the turbulence levels of the engine and the cascade are unknown, a precise comparison with reference 13 can not be made.

Comparison of temperature profiles and leading-edge heat-transfer coefficients shows that the results for the vane of this report, where the ratio $h_{g,eng}/h_{g,cas}$ in the leading-edge region was between 0.80 and 1.05, are in disagreement with values found in other investigations (refs. 1, 2, and 13). Therefore, it is felt that, as discussed in the section Comparison of Chordwise Temperature Distributions, a difference

did exist in the coolant-flow distribution of the engine vane and the cascade vane. And, because of this maldistribution of the coolant flow, the method of calculating heat-transfer coefficient ratios is invalid for this vane because it does not meet one of the previously stated requirements, that is, that the coolant Reynolds number (or coolant flow rate) at the leading edge must be the same in the engine and cascade vanes.

Vane Potential

The potential operating limits of the vane of this report are shown by figure 14. Thermocouple location 8 was the local "hotspot" of the engine vane, and the correlation constants for this thermocouple location were used in equation (16) to define the curves presented in figure 14. The limiting conditions are listed in table IV. The maximum wall temperature of 1280 K (1844° F) was dictated by the vane material Udimet 700. The vane design operating conditions are a turbine-inlet temperature and pressure of 1540 K (2312° F) and 29.5 newtons per square centimeter (42.8 psia), an inlet coolant temperature of 590 K (602° F), and a coolant- to gas-flow ratio of 0.05. As shown by figure 14 for the given design coolant conditions, the engine could be operated at a turbine-inlet temperature of 1590 K (2402° F). If the leading-edge geometry is redesigned as noted in the section Comparison of Chordwise Temperature Distributions, the vane potential will be considerably improved. Reference 8 shows that the turbine-inlet temperature would be approximately 1850 K (2870° F).

The lower curve of figure 14, for a coolant temperature of 810 K (998° F), describes the potential turbine-inlet temperature expected for supersonic flight conditions. At the design coolant- to gas-flow ratio of 0.05, the turbine-inlet temperature would be limited to 1490 K (2222° F). If the vane is redesigned the turbine-inlet temperature would be approximately 1680 K (2564° F).

CONCLUDING REMARKS

A comparison of engine and cascade vane data for the vane discussed in this report and a comparison of these trends with previous results for different vanes suggest that the coolant-flow distribution in the cascade vane differed markedly from the coolant-flow distribution in the engine vane and resulted in higher cascade leading-edge temperatures than expected. This difference is attributed to differences in the leading-edge exhaust plenum back pressure.

Results of previous studies indicate that the cascade and the engine vane data differ primarily on the gas side of the leading-edge region. This difference is attributed to

higher turbulence levels in the engine compared to the cascade, and this turbulence results in higher heat-transfer coefficients and higher temperatures at the leading edge of the engine vane.

It is concluded, from these observations, that the cascade can be used as a screening facility for the engine and can also be used as a tool for performing detailed heat-transfer studies provided those parameters that can and do differ between the two facilities are recognized. The critical gas-side parameters are the turbulence level, which affects the leading-edge heat-transfer coefficients; the turbine-inlet temperature; and the static-pressure distribution around the vane. The critical coolant-side parameters are those, such as the leading-edge back pressure, which could adversely affect the distribution of coolant to the various areas of the vane.

SUMMARY OF RESULTS

The heat-transfer characteristics of a chordwise-finned, impingement-cooled vane were investigated in both a modified J-75 turbojet research engine and a four-vane cascade. This investigation produced the following results:

1. Based on the average temperature difference ratio, the engine vane and the cascade vane performed the same for the conditions tested. In effect, the average vane temperatures were the same for a given gas and coolant temperature. However, the chordwise temperature profile presented in this report indicated the pressure surface of the engine vane was up to 90 K (162° F) hotter than similar positions on the cascade vane.

2. The average temperature difference ratio correlation and two empirical modifications of this correlation generally correlated the average vane temperatures within ±5 percent. Use of the modifications may not be justified because of the complexity and limited improvement of these correlations.

3. A comparison of gas-side heat-transfer coefficients of the engine vane and the cascade vane does not follow the results of previous investigations which report significantly higher heat-transfer coefficients around the leading edge of the engine vane. Stream turbulence is considered the primary cause of these increased coefficients for the engine vane. The inability to obtain a similar comparison in this report results from the necessity for having equal coolant-flow Reynolds numbers in both the cascade and engine vane leading edges in order to calculate the ratio of heat-transfer coefficients between the engine and cascade. The flow distributions in the vanes for the cascade and engine were believed to be different for the vane configuration tested.

4. Good agreement was obtained for calculated wall temperatures (based on one-dimensional heat flow and a leading-edge to trailing-edge coolant-flow split of 30 percent

to 70 percent) and experimental wall temperatures for the cascade vane. The comparisons were made at locations where chordwise and spanwise conduction components were at a minimum.

5. It was found that, at the design conditions for this vane and a maximum wall temperature at 1280 K (1844° F), this vane could be operated at a turbine-inlet temperature of 1590 K (2402° F) and a coolant temperature of 590 K (602° F). If the vane were redesigned to optimize the leading-edge geometry, the potential turbine-inlet temperature would be 1850 K (2870° F).

Lewis Research Center,
National Aeronautics and Space Administration,
Cleveland, Ohio, April 24, 1972,
764-74.

REFERENCES

1. Gladden, Herbert J.; Livingood, John N. B.; and Gaunter, Daniel J.: Comparison of Temperature Data Between a Four-Vane Static Cascade and a Research Gas Turbine Engine for a Chordwise-Finned, Impingement- and Film-Cooled Vane. NASA TM X-2477, 1972.

2. Gladden, Herbert J.; Gauntner, Daniel J.; and Livingood, John N. B.: Analysis of Heat-Transfer Tests of an Impingement-Convection- and Film-Cooled Vane in a Cascade. NASA TM X-2376, 1971.

3. Dengler, Robert P.; Yeh, Frederick C.; Gauntner, James W.; and Fallon, Gerald E.: Engine Investigation of Air-Cooled Turbine Rotor Blade Incorporating Impingement-Cooled Leading Edge, Chordwise Passages, and a Slotted Trailing Edge. NASA TM X-2526, 1972.

4. Gauntner, James W.; Lane, Jan M.; Dengler, Robert P.; and Hickel, Robert O.: Experimental Heat-Transfer Results of a Chordwise Finned Turbine Vane with Impingement, Film, and Convection Cooling. NASA TM X-2472, 1972.

5. Calvert, Howard F.; Cochran, Reeves P.; Dengler, Robert P.; Hickel, Robert O.; and Norris, James W.: Turbine Cooling Research Facility. NASA TM X-1927, 1970.

6. Crowl, Robert J.; and Gladden, Herbert J.: Methods and Procedures for Evaluating, Forming, and Installing Small-Diameter Sheathed Thermocouple Wire and Sheathed Thermocouples. NASA TM X-2377, 1971.

7. Gladden, Herbert J.; and Livingood, John N. B.: Procedure for Scaling of Experimental Turbine Vane Airfoil Temperatures from Low to High Gas Temperature. NASA TN D-6510, 1971.

8. Yeh, Frederick C.; Gladden, Herbert J.; and Gauntner, James W.: Comparison of Heat-Transfer Characteristics of Three Cooling Configurations for Air-Cooled Turbine Vanes Tested in a Turbojet Engine. NASA TM X-2580, 1972.

9. Stepka, Francis S.: Considerations of Turbine Cooling Systems for Mach 3 Flight. NASA TN D-4491, 1968.

10. Esgar, Jack B.; Colladay, Raymond S.; and Kaufman, Albert: An Analysis of The Capabilities and Limitations of Turbine Air Cooling Methods. NASA TN D-5992, 1970.

11. Simoneau, R. J.; and Hendricks, R. C.: A Simple Equation for Correlating Turbulent Heat Transfer to a Gas. Paper 64-HT-36, ASME, Aug. 1964.

12. Jenkins, D. E.; and Metzger, C. W.: Local Heat Transfer Characteristics of Concave Cylindrical Surfaces Cooled by Impinging Slot Jets and Lines of Circular Jets with Spacing Ratios 1.25 to 6.67. Rep. TR-694, Arizona State Univ., May, 1969.

13. Dyban, Ye. P.; and Kurosh, V. D.: Heat Transfer at The Leading Edge of a Turbine Blade. Heat Transfer - Soviet Research, vol. 2, no. 1, Jan. 1970, pp. 36-40.

TABLE I. - CASCADE OPERATING CONDITIONS

Average turbine-inlet temperature, T_{Ti}		Average turbine-inlet pressure, p_{Ti}		Average coolant inlet temperature, T_{ci}		Coolant- to gas-temperature ratio	Coolant- to gas-flow ratio, $\dot{w}_c/\dot{w}_g$	Symbols used in figures
K	^{o}F	N/cm^2	psia					
760	909	12.95	18.8	310	98	0.408	0.02 to 0.086	○
760	909	26.4	38.3	310	98	.408	0.019 to 0.127	□
760	909	39.8	57.8	310	98	.408	0.023 to 0.117	△
760	909	26.4	38.3	425	305	.559	0.023 to 0.10	⬠
1400	2060	29.5	42.8	700	800	.50	0.024 to 0.113	◇
1400	2060	29.5	42.8	810	998	.579	0.021 to 0.129	⬠
1540	2312	29.5	42.8	310	98	.201	0.052 to 0.121	▽
1540	2312	29.5	42.8	600	620	.39	0.046 to 0.113	◁
1540	2312	59.0	85.6	600	620	.39	0.041 to 0.081	⬠
1650	2510	29.7	43.1	310	98	.188	0.066 to 0.120	▷

TABLE II. - ENGINE OPERATING CONDITIONS

Average compressor inlet temperature		Average turbine-inlet temperature, T_{Ti}		Engine speed, rpm	Average coolant inlet temperature, T_{ci}		Coolant- to gas-temperature ratio	Coolant- to gas-flow ratio, $\dot{w}_c/\dot{w}_g$	Symbols used in figures
K	^{o}F	K	^{o}F		K	^{o}F			
305	89	1260	1808	7600 to 7860	310	98	0.246	0.027 to 0.125	⬠
455	359	1375	2014	6750 to 7760	310	98	.226	0.038 to 0.125	◇
455	359	1530	2294	8250	310	98	.203	0.057 to 0.121	▽
455	359	1640	2493	8690	310	98	.189	0.087 to 0.108	▷
455	359	1370	2006	7750 to 7890	700	800	.511	0.028 to 0.111	◇
455	359	1530	2294	8160 to 8450	480	404	.314	0.046 to 0.127	◺

TABLE III. - COMPARISON OF LEADING-EDGE HEAT-TRANSFER COEFFICIENTS FOR THREE VANES TESTED IN ENGINE AND CASCADE

Distance from stagnation point, deg	Vane of this report	Vane of ref. 1	Vane of ref. 2 (a)
	Ratio of heat-transfer coefficients, $h_{g,eng}/h_{g,cas}$		
Suction surface			
~60	1.05	1.45	(b)
~45	(b)	(b)	1.50
Stagnation point			
0	0.8	1.30	1.30
Pressure surface			
~45	(b)	(b)	----
~60	1.00	----	(b)

[a]Unpublished engine data were utilized for this comparison.
[b]Thermocouples were not located at this position.

TABLE IV. - OPERATING LIMITS WHICH DEFINE VANE POTENTIAL

Coolant inlet temperature, T_{ci}		Maximum wall temperature, $T_{w,max}$	
K	^{o}F	K	^{o}F
810	998	1280	1844
590	602	1280	1844

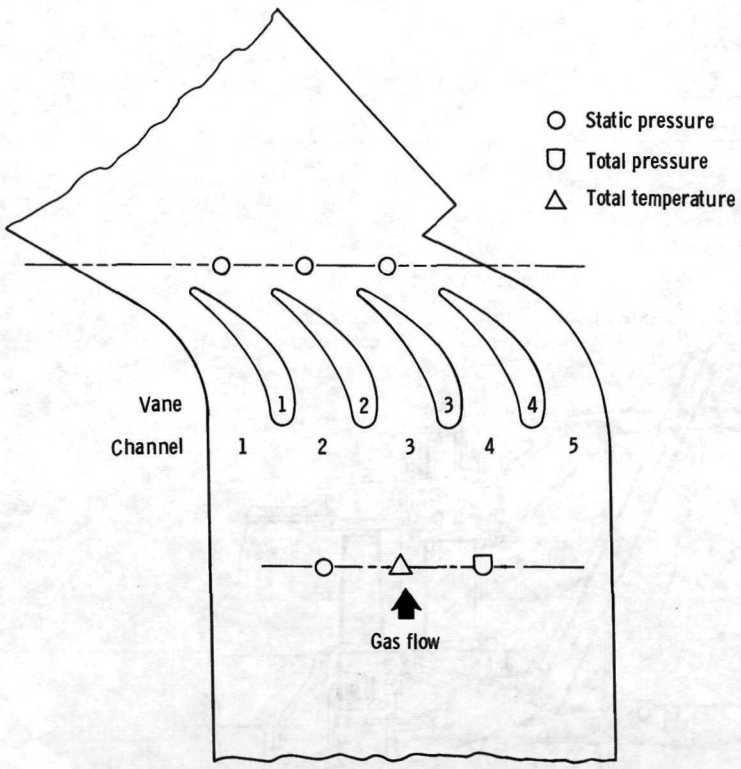

(a) Plan view

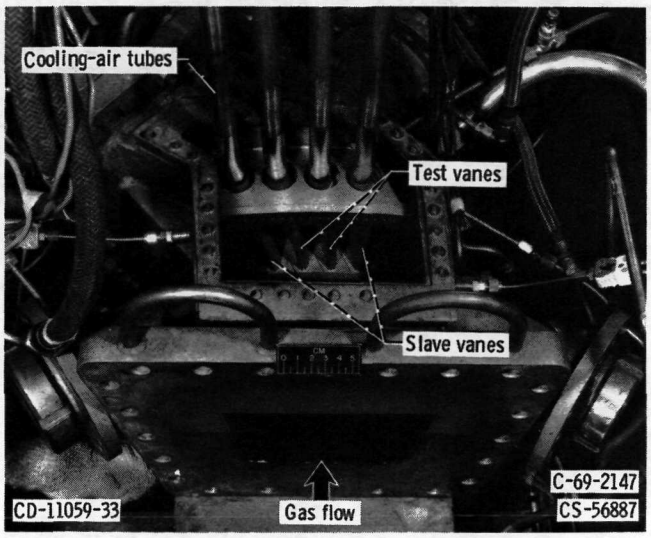

(b) Cascade test section with cover removed.

Figure 1. - Static cascade.

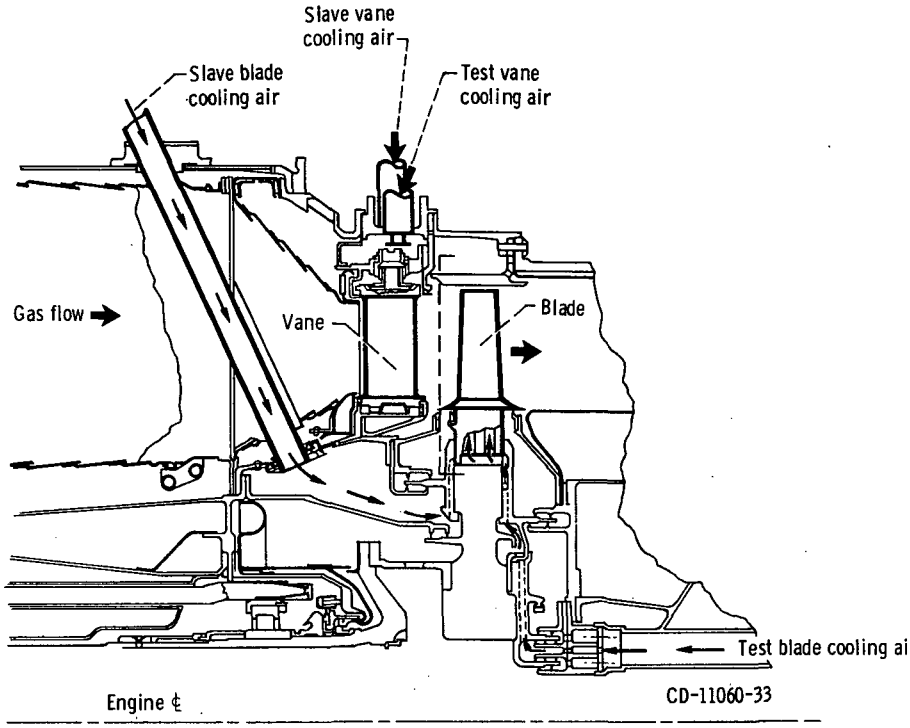

Figure 2. - Turbine cooling research engine.

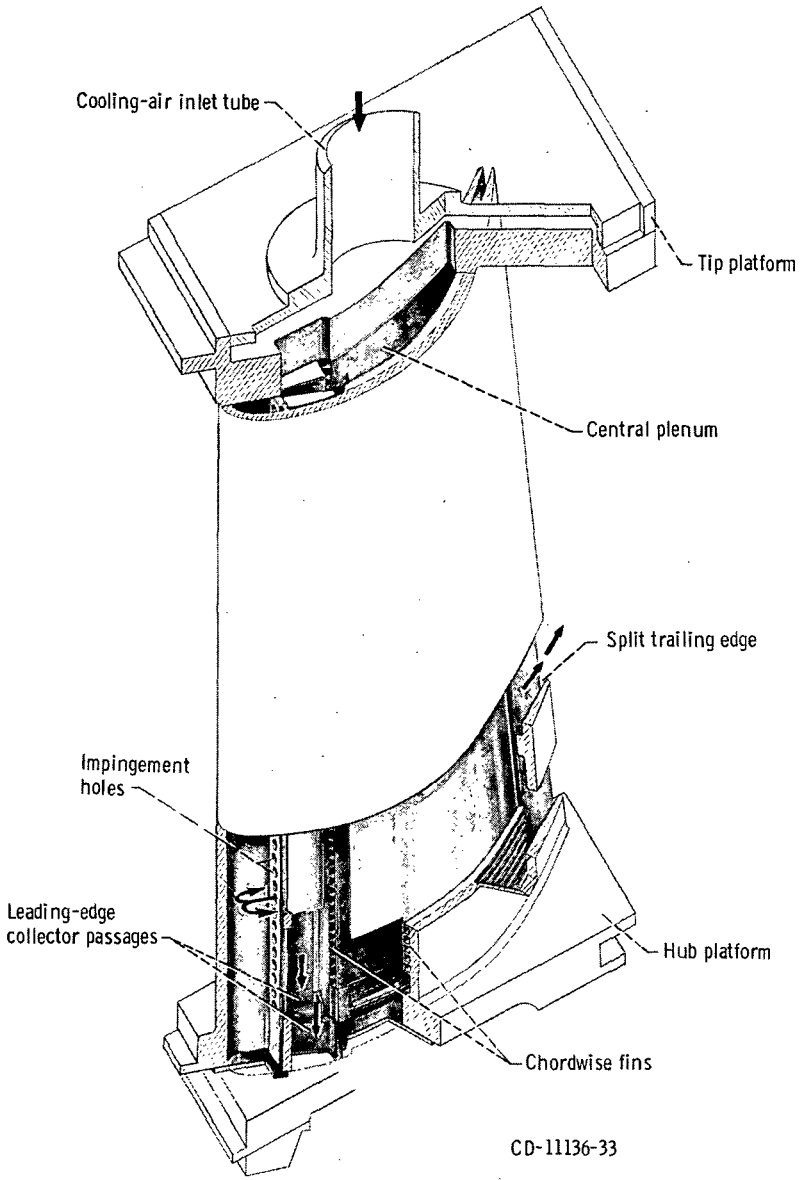

Figure 3. - Cutaway drawing of test vane.

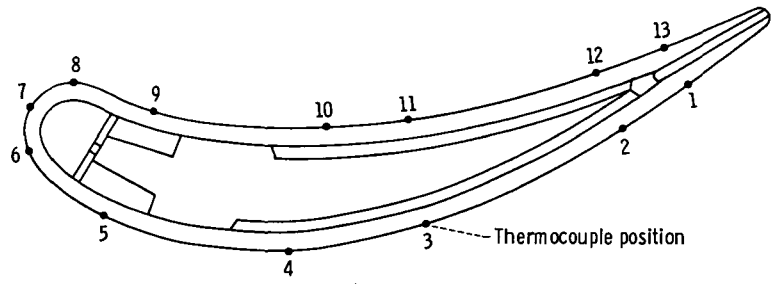

Figure 4. - Composite of midspan thermocouple locations on test vanes installed in cascade and engine.

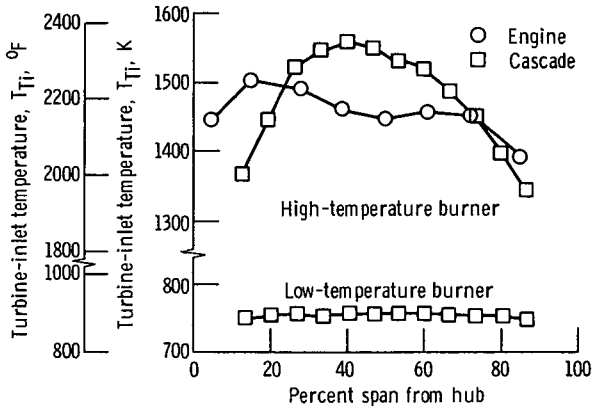

Figure 5. - Typical radial turbine-inlet temperature distribution for engine and two cascade burners.

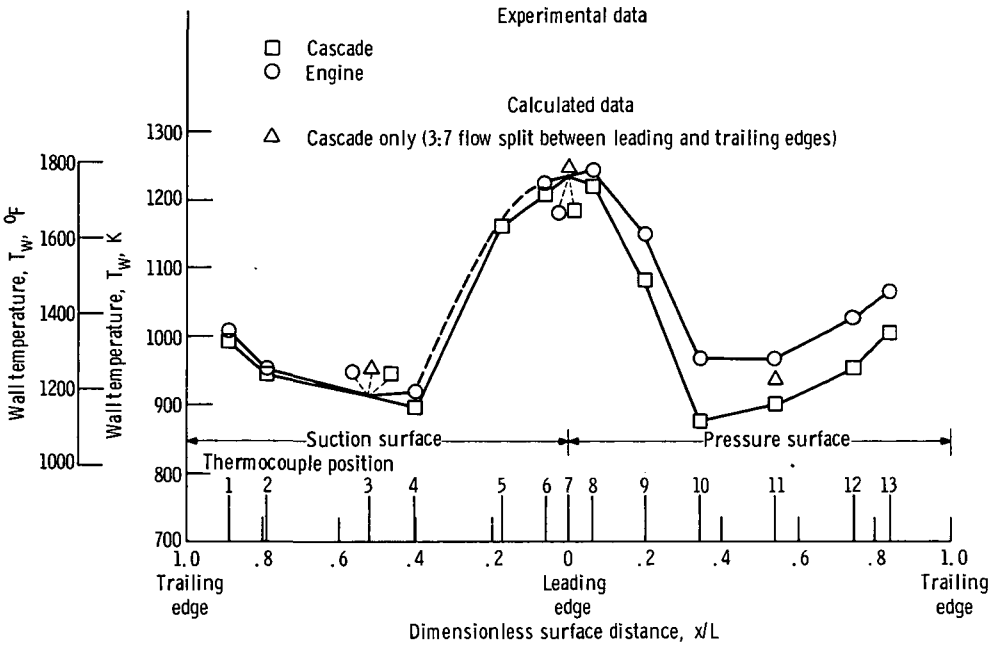

Figure 6. - Experimental midspan wall temperature profiles for cascade and engine test vanes. Cascade conditions: turbine-inlet temperature, 1540 K (2310° F); coolant inlet temperature, 600 K (620° F); coolant- to gas-flow ratio, 0.064. Engine conditions: turbine-inlet temperature, 1525 K (2285° F); coolant inlet temperature, 600 K (620° F); coolant- to gas-flow ratio, 0.061.

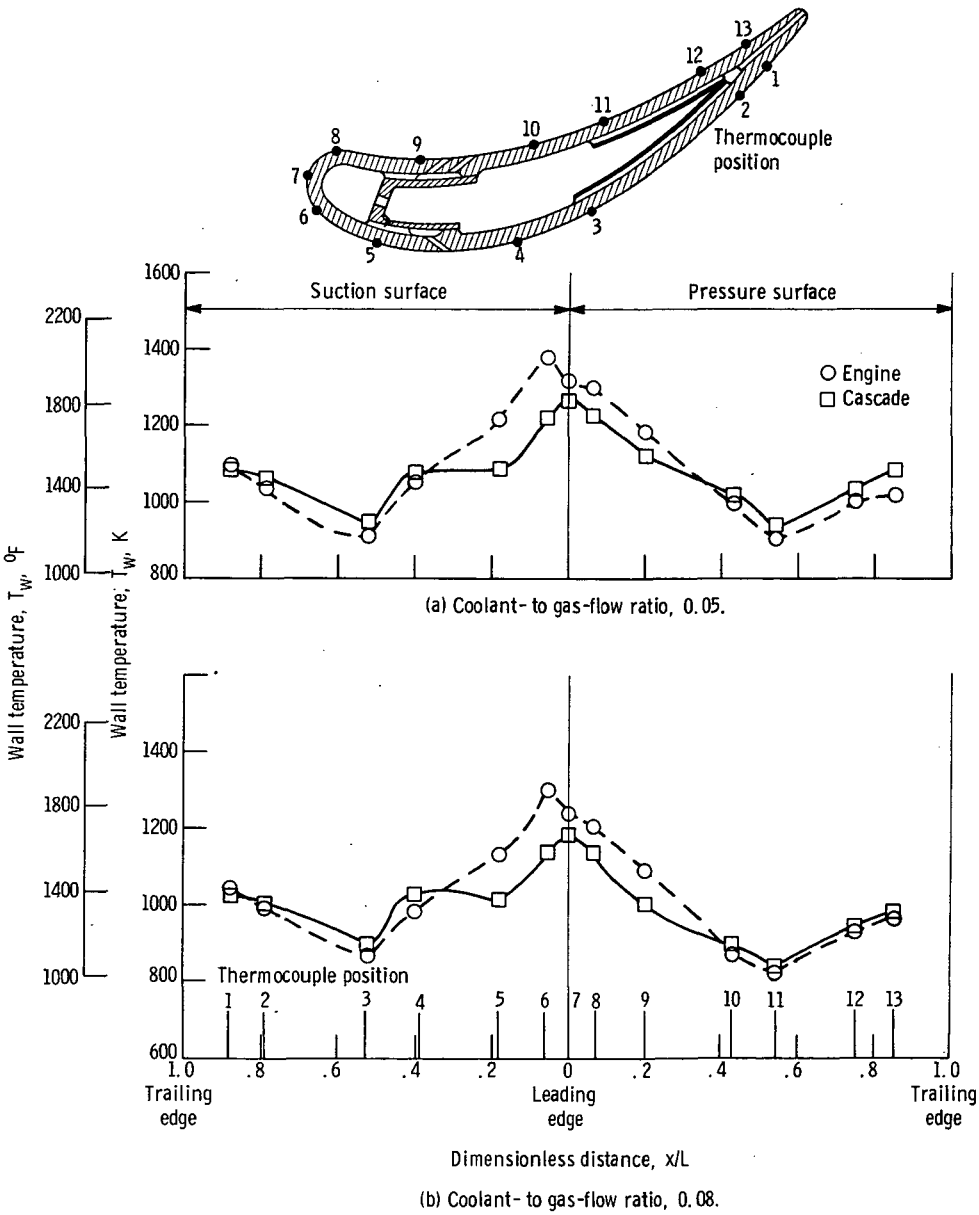

(a) Coolant- to gas-flow ratio, 0.05.

(b) Coolant- to gas-flow ratio, 0.08.

Figure 7. - Comparison of midspan chordwise temperature distributions for reference 1 vane for cascade and engine. Turbine-inlet temperature, 1533 K (2300° F); coolant temperature, 589 K (600° F).

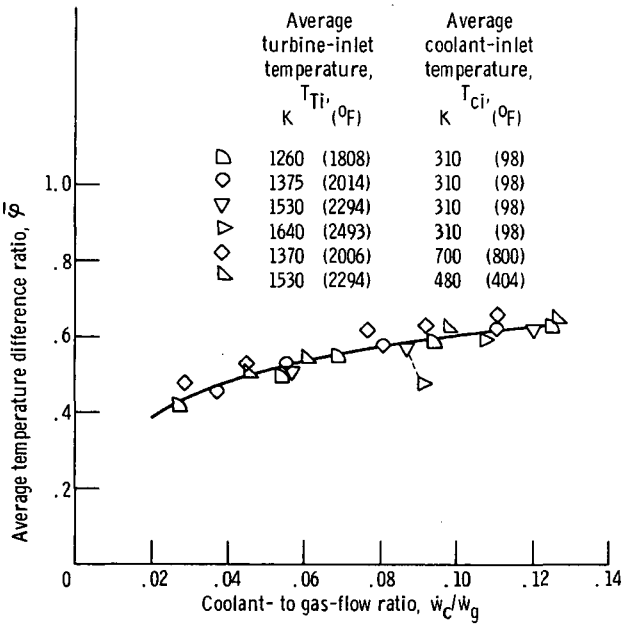

Figure 8. - Average midspan temperature correlation for engine data. Conditions listed in table II; $\bar{\varphi}_{eng} = \frac{1}{1 + 0.18(\dot{w}_c/\dot{w}_g)^{-0.55}}$.

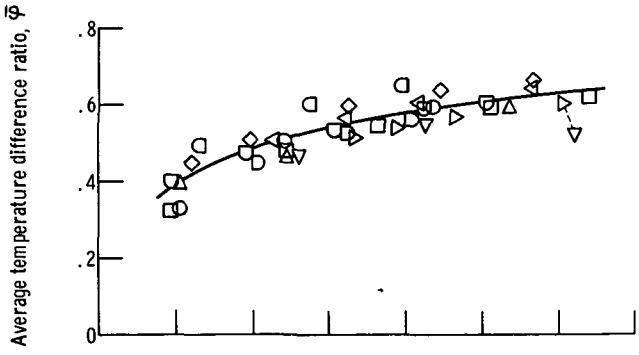

(a) Cascade average correlation; $\overline{\varphi}_{cas} = \frac{1}{1 + 0.18(\dot{w}_c/\dot{w}_g)^{-0.55}}$.

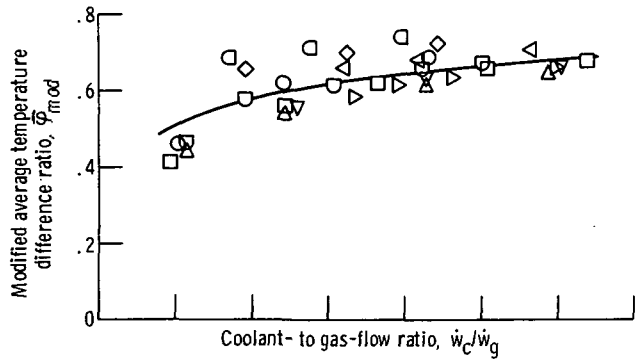

	Average turbine-inlet temperature, T_{Ti}, K	(^{o}F)	Average coolant-inlet temperature, T_{ci}, K	(^{o}F)
○	760	(909)	310	(98)
□	760	(909)	310	(98)
△	760	(909)	310	(98)
▢	760	(909)	425	(305)
◇	1400	(2060)	700	(800)
▢	1400	(2060)	810	(998)
▽	1540	(2312)	310	(98)
◁	1540	(2312)	600	(620)
▢	1540	(2312)	600	(620)
▷	1650	(2510)	310	(98)

(b) Cascade correlation modified to average coolant temperature basis; $\overline{\varphi}_{mod} = \frac{1}{1 + 0.20(\dot{w}_c/\dot{w}_g)^{-0.41}}$.

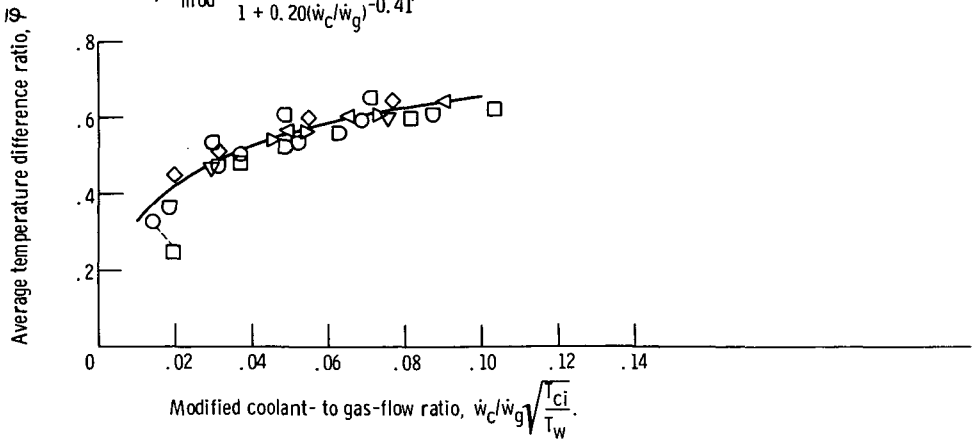

(c) Cascade correlation modified by coolant- to wall-temperature ratio; $\overline{\varphi} = \frac{1}{1 + 0.13(\dot{w}_c/\dot{w}_g\sqrt{T_{ci}/\overline{T}_w})^{-0.60}}$.

Figure 9. - Average midspan temperature correlation of cascade vane data for three different correlation methods. Conditions listed in table I.

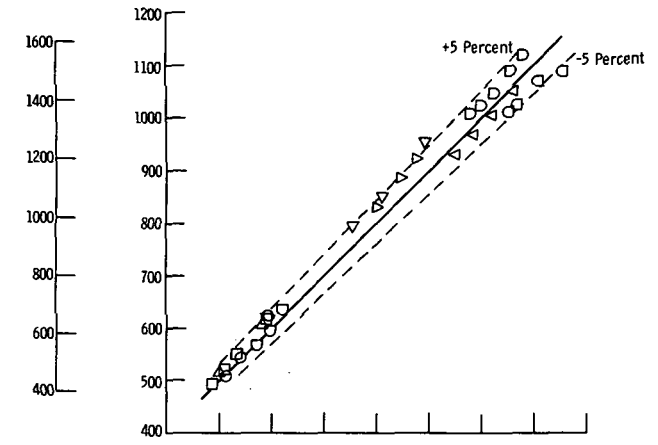

(a) Temperatures calculated by average temperature difference ratio correlation.

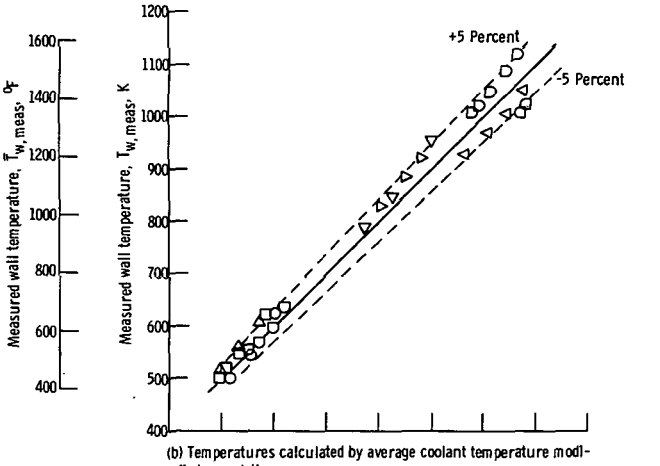

	Average turbine-inlet temperature, T_{Ti}, K	(°F)	Average coolant-inlet temperature, T_{ci}, K	(°F)
○	760	(909)	310	(98)
□	760	(909)	310	(98)
△	760	(909)	310	(98)
▢	760	(909)	425	(305)
◇	1400	(2060)	700	(800)
▢	1400	(2060)	810	(998)
◁	1540	(2312)	310	(98)
◁	1540	(2312)	600	(620)
▢	1540	(2312)	600	(620)
▷	1650	(2510)	310	(98)

(b) Temperatures calculated by average coolant temperature modified correlation.

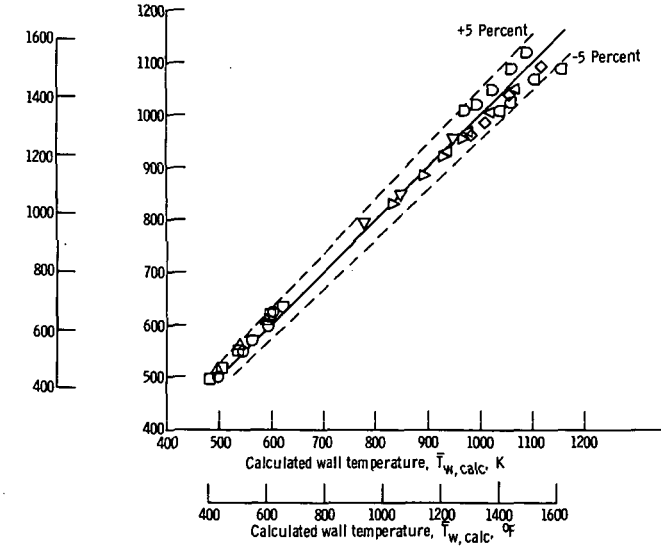

(c) Temperatures calculated by temperature ratio modified correlation.

Figure 10. - Comparison of average experimental wall temperature and average wall temperature determined by correlations. Conditions listed in table I.

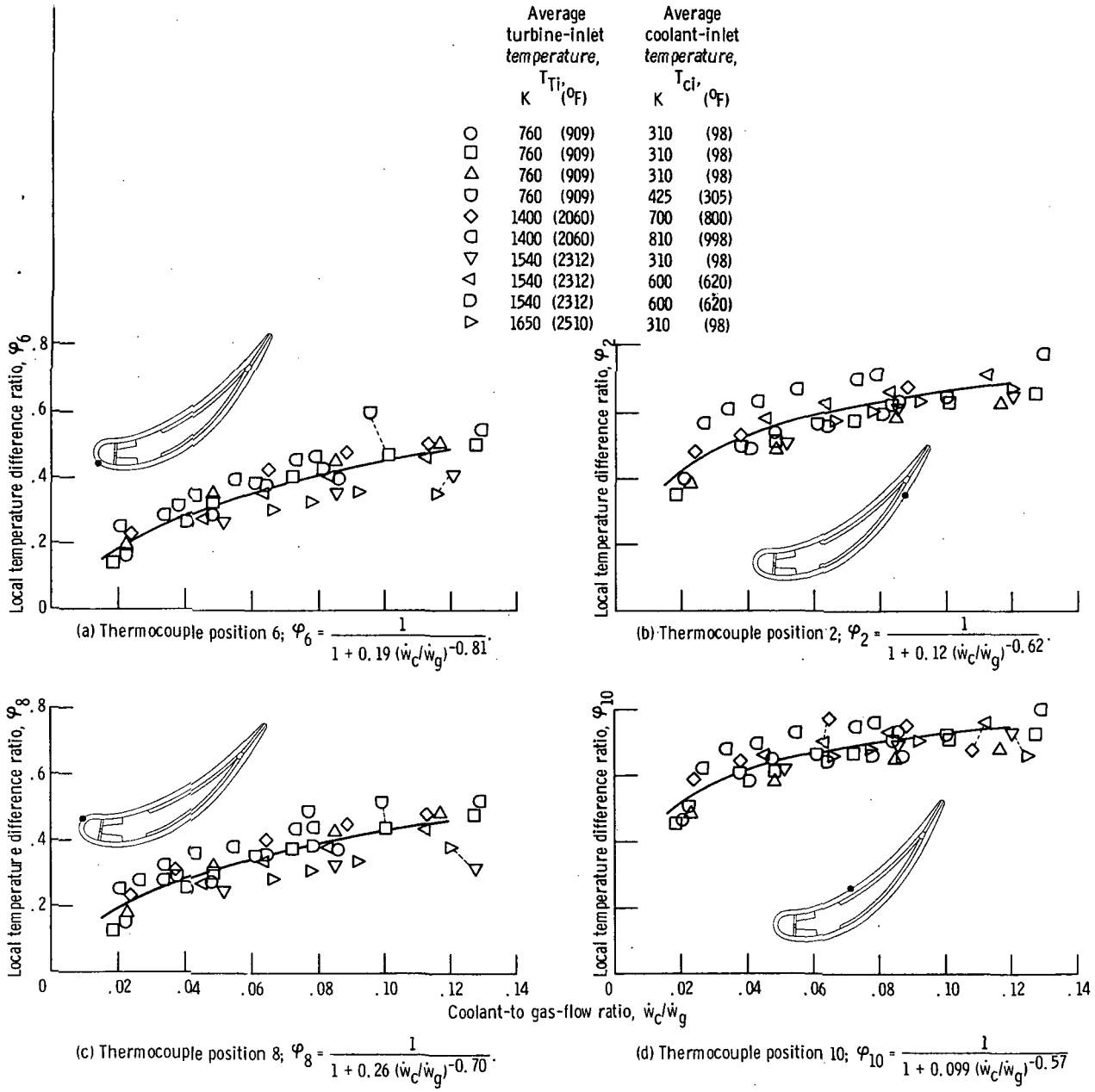

Figure 11. - Local temperature correlation of cascade data. Conditions listed in table I.

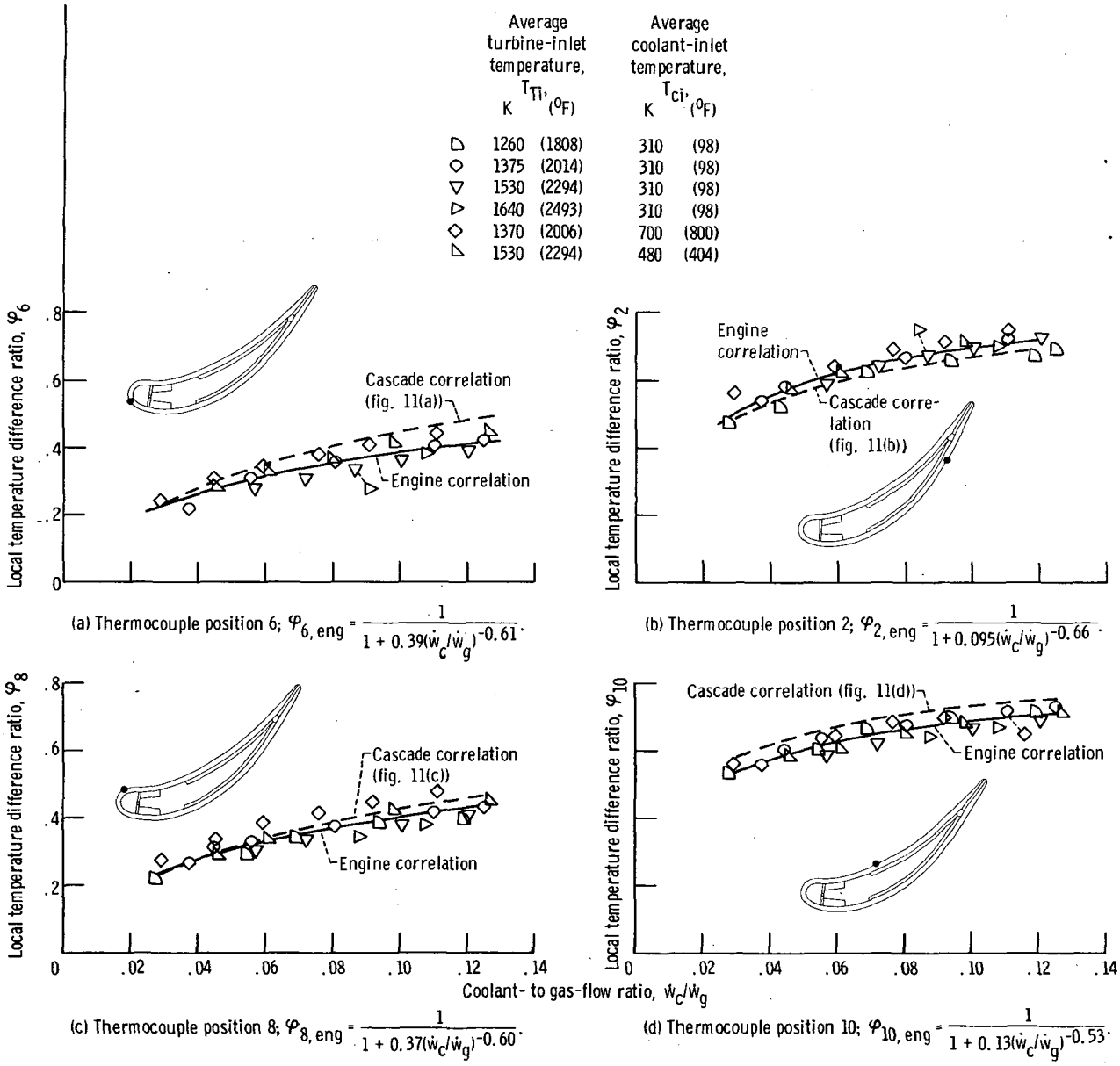

(a) Thermocouple position 6; $\varphi_{6,eng} = \frac{1}{1 + 0.39(\dot{w}_c/\dot{w}_g)^{-0.61}}$.

(b) Thermocouple position 2; $\varphi_{2,eng} = \frac{1}{1 + 0.095(\dot{w}_c/\dot{w}_g)^{-0.66}}$.

(c) Thermocouple position 8; $\varphi_{8,eng} = \frac{1}{1 + 0.37(\dot{w}_c/\dot{w}_g)^{-0.60}}$.

(d) Thermocouple position 10; $\varphi_{10,eng} = \frac{1}{1 + 0.13(\dot{w}_c/\dot{w}_g)^{-0.53}}$.

Figure 12. - Comparison of local correlations for engine and cascade. Conditions listed in table II.

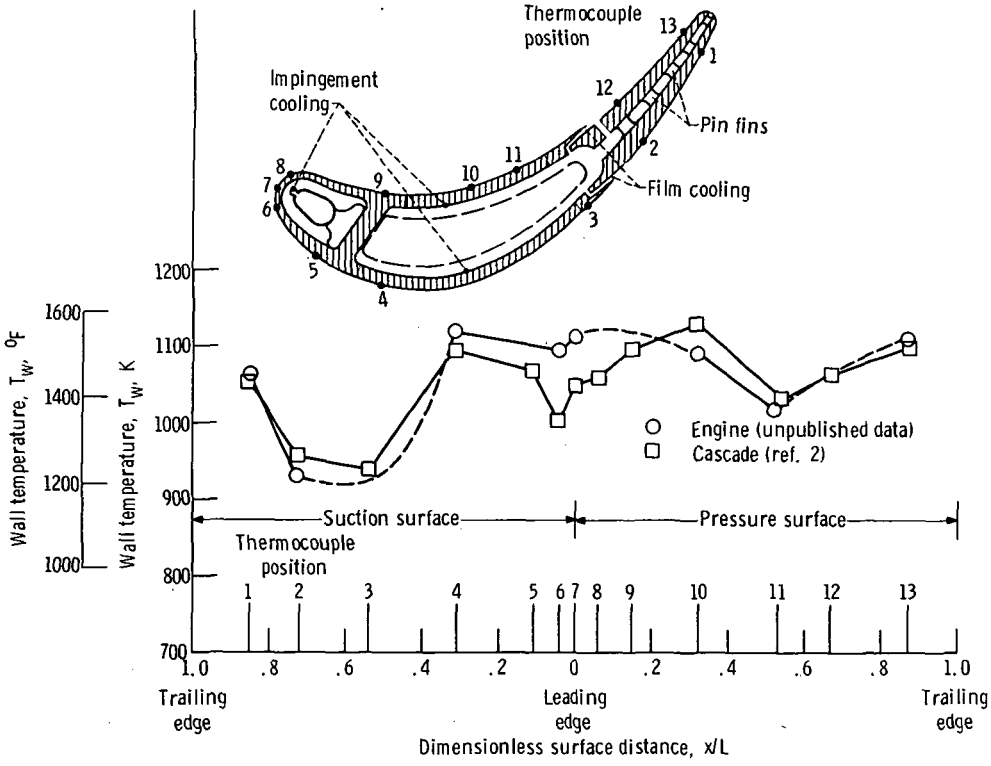

Figure 13. - Comparison of engine and cascade experimental wall temperature profiles for reference 2 vane. Cascade conditions: turbine-inlet temperature, 1644 K (2500° F); coolant inlet temperature, 298 K (76° F); coolant- to gas-flow ratio, 0.042. Engine conditions: turbine-inlet temperature, 1614 K (2445° F); coolant inlet temperature, 313 K (104° F); coolant- to gas-flow ratio, 0.045.

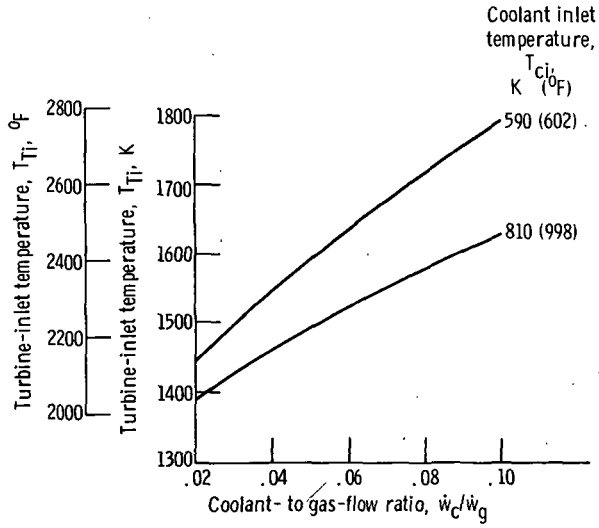

Figure 14. - Potential turbine-inlet temperature operating limit for maximum wall temperature of 1280 K (1844° F). Calculation based on engine thermocouple position 8 and equation (16).

"The aeronautical and space activities of the United States shall be conducted so as to contribute . . . to the expansion of human knowledge of phenomena in the atmosphere and space. The Administration shall provide for the widest practicable and appropriate dissemination of information concerning its activities and the results thereof."

—NATIONAL AERONAUTICS AND SPACE ACT OF 1958

NASA SCIENTIFIC AND TECHNICAL PUBLICATIONS

TECHNICAL REPORTS: Scientific and technical information considered important, complete, and a lasting contribution to existing knowledge.

TECHNICAL NOTES: Information less broad in scope but nevertheless of importance as a contribution to existing knowledge.

TECHNICAL MEMORANDUMS: Information receiving limited distribution because of preliminary data, security classification, or other reasons.

CONTRACTOR REPORTS: Scientific and technical information generated under a NASA contract or grant and considered an important contribution to existing knowledge.

TECHNICAL TRANSLATIONS: Information published in a foreign language considered to merit NASA distribution in English.

SPECIAL PUBLICATIONS: Information derived from or of value to NASA activities. Publications include conference proceedings, monographs, data compilations, handbooks, sourcebooks, and special bibliographies.

TECHNOLOGY UTILIZATION PUBLICATIONS: Information on technology used by NASA that may be of particular interest in commercial and other non-aerospace applications. Publications include Tech Briefs, Technology Utilization Reports and Technology Surveys.

Details on the availability of these publications may be obtained from:

SCIENTIFIC AND TECHNICAL INFORMATION OFFICE

NATIONAL AERONAUTICS AND SPACE ADMINISTRATION

Washington, D.C. 20546